Published in final edited form as:
J Immunol. 2009 July 1; 183(1): 578–592. doi:10.4049/jimmunol.0900120.

Differential regulation of P2X7 receptor activation by extracellular NAD and ecto-ARTs in murine macrophages and T cells

Shiyuan Hong[*], **Nicole Schwarz**[**], **Anette Brass**[**], **Michel Seman**[***], **Friedrich Haag**[**], **Friedrich Koch-Nolte**[**], **William P. Schilling**[*], and **George R. Dubyak**[*]

[*] Department of Physiology and Biophysics, Case Western Reserve University School of Medicine, Cleveland OH, USA

[**] Institute of Immunology, University Hospital, Hamburg, Germany

[***] University of Rouen, Rouen, France

Abstract

Extracellular NAD induces the ATP-independent activation of the ionotropic P2X7 purinergic receptor (P2X7R) in murine T lymphocytes via a novel covalent pathway involving ADP-ribosylation of arginine residues on the P2X7R ecto-domain. This modification is catalyzed by ART2.2, a GPI-anchored ADP-ribosyltransferase (ART) that is constitutively expressed in murine T cells. We previously reported that ART2.1, a related ecto-ART, is up-regulated in inflammatory murine macrophages that constitutively express P2X7R. Thus, we tested the hypothesis that extracellular NAD acts via ART2.1 to regulate P2X7R function in murine macrophages. Co-expression of the cloned murine P2X7R with ART2.1 or ART2.2 in HEK293 cells verified that P2X7R is an equivalent substrate for ADP-ribosylation by either ART2.1 or ART2.2. However, in contrast with T cells, stimulation of macrophages or HEK293 cells with NAD alone did not activate the P2X7R. Rather, NAD potentiated ATP-dependent P2X7R activation as indicated by a left-shift in the ATP dose-response relationship. Thus, extracellular NAD regulates the P2X7R in both macrophages and T cells but via distinct mechanisms. While ADP-ribosylation is sufficient to gate P2X7R channel opening in T cells, this P2X7R modification in macrophages does not gate the channel but decreases the threshold for gating in response to ATP binding. These findings indicate that extracellular NAD and ATP can act synergistically to regulate P2X7R signaling in murine macrophages and also suggest that the cellular context in which P2X7R signaling occurs differs between myeloid versus lymphoid leukocytes.

Introduction

The P2X7 purinergic receptor (P2X7R) is an ATP-gated non-selective cation channel that is predominantly expressed in cells of hematopoietic origin including macrophages and T lymphocytes (1). The subunit structure of this 595 amino acid receptor includes two transmembrane segments, an intracellular N-terminus, an intracellular C-terminus, and a large

Address correspondence and reprint requests to: George R. Dubyak, Ph.D., Department of Physiology and Biophysics, Case Western Reserve University School of Medicine, 10900 Euclid Avenue, Cleveland OH, 44120, george.dubyak@case.edu, Phone (216)368-5523, FAX (216)368-3952.

extracellular loop (47–329 AA) which contain presumed site(s) for ATP binding (2). Three of these P2X7 subunits assemble to form the trimeric P2X7R channel (3). Stimulation of the P2X7R with extracellular ATP rapidly triggers increased Na^+, K^+, and Ca^{2+} fluxes across the plasma membrane (2), followed by the delayed induction of a non-selective pore which facilitates the permeation of molecules up to 900 Da in mass (4). Given its expression in myeloid and lymphoid leukocytes, many studies have identified roles for the P2X7R in the regulation of various pro-inflammatory and immune responses (reviewed in (5–7).

An unusual and defining feature of the P2X7R is its high threshold for activation by extracellular ATP (EC_{50} ~ 500 μM); this contrasts with much lower activation thresholds for the other six members of the P2X family (EC_{50} ~ 10 μM) (1,8,9). Intracellular ATP concentration is only 3–5 mM and most cells express significant ecto-ATPase activities. Thus, it is unlikely that submillimolar levels of extracellular ATP can be sustained for significant durations within interstitial tissue compartments except perhaps during massive lysis of host cells or killing of invading pathogens. Clearly, the P2X7R is activated within *in situ* inflammatory loci or during normal development as indicated by the reduced levels of cytokines that accumulate within inflamed foot pads of P2X7R knockout mice (10) as well as the marked changes in bone density during aging of these mice (11). Autocrine activation of P2X7R via release of endogenous ATP has been recently reported in human monocytes in response to LPS stimulation of TLR4 signaling (12,13), and in T cells in response to antibody stimulation of TCR signaling cascades (14). This released ATP may accumulate within diffusion-restricted microdomains of the cell surface, such as caveolar or nascent endosomal invaginations, not readily accessible to the bulk extracellular medium.

However, physiological P2X7R activation may involve modes of regulation in addition to autocrine stimulation. One is allosteric modulation of ATP affinity via conformational changes in P2X7 trimeric channels produced by local biophysical conditions such as pH, ionic composition (15–17), or membrane lipid composition (18). For example, lysophosphatidylcholine and other lysolipids reduce the threshold level of ATP required for P2X7R-dependent Ca^{2+} influx and pore formation in murine microglia (19). Another type of regulation involves the gating of P2X7R channels by mechanisms independent of reversible ATP binding. Notably, extracellular NAD induces the ATP-independent activation of P2X7R in murine T lymphocytes via a novel covalent pathway involving ADP-ribosylation of arginine residues on the P2X7R ecto-domain (20–22).

The ADP-ribosylation of P2X7R is catalyzed by ART2, a GPI-anchored ADP-ribosyltransferase (ART) constitutively expressed on the cell surface of murine T cells (23–25). ART2 belongs to a family of ecto-enzymes which utilize extracellular NAD to transfer the ADP-ribose moiety to substrate proteins (26). ART2 mediates P2X7R transactivation via ADP-ribosylation of the R125 residue within the extracellular loop of the receptor (21). This covalent modification apparently mimics the conformational changes in P2X7R induced by non-covalent ATP binding and triggers both Ca^{2+} influx and the secondary non-selective pore permeable to fluorescent dyes. The NAD- and ART2-dependent activation of P2X7R consequently induces phosphatidylserine exposure on T cell surfaces, increased shedding of CD62L, and acceleration of T-cell death. Other studies have shown that extracellular NAD induces P2X7R activation in *in vivo* models of immune and inflammatory responses (21,27, 28).

ART2 includes two isoforms, ART2.1 and ART2.2, which are encoded by tandem genes (*Art2a* and *Art2b*) located on murine chromosome 7 (26). Although ART2.1 is functionally and structurally similar to ART2.2, it contains two additional cysteine residues (Cys-80 and Cys-201) that readily form a disulfide bond which allosterically suppresses catalytic activity (29). This inhibited state of ART2.1 is reversed by extracellular thiol reductants, such as

exogenous dithiolthreitol or the endogenous cysteine and glutathione released by inflamed or damaged tissues (30,31). T cells from most inbred mouse strains (e.g. BALB/c) natively express both ART2.1 and ART2.2 (25,32–34). However, the latter isoform is sufficient for NAD-induced P2X7R activation and cell death because these responses occur in the absence of extracellular thiol reductants and in T cells from C57BL/6 mice which express a mutated *Art2a* gene and no functional ART2.1 protein (20,35).

Although the NAD-induced, ART2-dependent mechanism is clearly a major pathway for P2X7R activation in mouse T lymphocytes, it is unclear whether this mechanism is operative in macrophages, another class of leukocytes which natively express P2X7R at high levels. Relevant to this issue, we have reported the inducible expression of ART2.1, but not ART2.2, in murine bone marrow-derived macrophages (BMDM) stimulated by multiple inflammatory factors(36). This prompted us to examine the role of ART2.1 as a regulator of P2X7 receptors natively expressed in murine macrophages or heterologously expressed in HEK293 cells. We we demonstrate that co-expression of the murine P2X7R with ART2.1 or ART2.2 in HEK293 cells facilitates similar NAD-driven ADP-ribosylation of the receptor. However, NAD stimulation of P2X7R in macrophages or HEK293 cells is not sufficient to activate the receptor. Rather, the NAD/ART2-dependent modification of the P2X7R potentiates the ability of ATP to activate the receptor as indicated by a left-shift in the ATP dose-response relationship. Thus, extracellular NAD acts to regulate the ionotropic P2X7R in both macrophages and T cells but via distinct mechanisms on the gating of channel activity. These observations support a role for extracellular NAD in the regulation of P2X7R-dependent inflammatory responses in macrophages and additionally suggest that the cellular context (i.e. myeloid vs. lymphoid cells) dictates the outcome of signaling through the P2X7R.

Materials and Methods

Materials

Recombinant murine interferon-γ (IFN-γ) was from Boehringer Mannheim Biochemica and recombinant murine interferon-β (IFN-β) from US Biologicals. LPS (E.Coli serotype 01101:B4) was from List Biological Laboratories. ATP, NAD, etheno-NAD (εNAD), ADP-ribose (ADP-R), reduced glutathione (GSH), and TRIzol were from Sigma-Aldrich. Oligo dT primer was from Promega. AMV reverse transcriptase was from Roche. Tag DNA polymerase was from New England Biolabs. The 1G4 mouse monoclonal antibody (a generous gift from Dr. Regina Santella, Columbia University) was prepared as previously described (36). Fura2-AM, ethidium bromide, APC-conjugated Annexin-V and YO-PRO-1 were from Molecular Probes Inc. The anti-P2X7R K1G antibody and monoclonal antibodies directed against mouse ART2.1 or ART2.2 were generated and used as recently described (37). BALB/c, C57BL/6, and NZW mice were purchased from Taconic, Inc. P2X7R$^{-/-}$ mice were originally provided by Pfizer Global Research and Development, Pfizer Inc. and then backcrossed into a pure C57BL/6 background for >12 generations from a P2X7R$^{-/-}$ mouse strain described previously (38). All experiments and procedures involving mice were approved by the Institutional Animal Use and Care Committees of Case Western Reserve University or Hamburg University Hospital.

Cell culture and animals

Bone marrow-derived macrophages (BMDM) and splenocytes isolated from BALB/c, C57BL/6, NZW, or P2X7R−/− mice were prepared as previously described (36). Bac1.2F5 murine macrophages were cultured in DMEM (Sigma-Aldrich) supplemented with 25% L cell-conditioned medium, 15% calf serum (HyClone Laboratories), 100 U/ml penicillin, and 100 μg/ml streptomycin (Invitrogen Life Technologies) in the presence of 10% CO_2. RAW264.7 macrophages were cultured in DMEM supplemented with 10% calf serum, 100 U/ml penicillin,

and 100 μg/ml streptomycin in the presence of 10% CO_2. Where indicated, BMDM or the macrophage cell lines (Bac1.2F5; RAW264.7) were primed for 24 hr with either LPS (100 ng/ml), IFN-γ, (100 U/ml), or IFN-β (100 U/ml) to induce an inflammatory phenotype and up-regulation of ART2.1 expression. Murine BW5147 T lymphoma cells were maintained in RPMI 1640 supplemented with 10% calf serum and 1% penicillin-streptomycin in the presence of 5% CO_2. Wildtype HEK293 cells were cultured in DMEM supplemented with 10% calf serum and 1% penicillin-streptomycin in the presence of 10% CO_2. HEK293 cells stably transfected with either the wildtype murine P2X7R (HEK-mP2X7 cells) or the mutant R276K P2X7R (HEK-mP2X7-R276K cells) were selected and maintained in DMEM supplemented with 400 μg/ml G418 or 10 μg/ml Blasticidin. The ART2 plasmids were transiently transfected into HEK P2X7R cells using cells seeded at 6×10^5 per 35mm dishes 24 hours before transient transfection. The cells were transfected using Polyfect reagent (Qiagen) with 2.5 ug plasmid DNA per dish followed by incubation at 37°C for 36 hrs before experiments.

RT-PCR Analyses

Total RNA was extracted using TRIzol; all primers and PCR conditions for ecto-ARTs, iNOS, IFN-β and GAPDH were prepared and used as previously described(36). The PCR amplicons were separated by 1.5 % agarose gel electrophoresis and visualized by ethidium bromide staining; the resulting fluorescence images were recorded with a BioRad Gel Doc 1000 system.

1G4 monoclonal antibody-based assay of ART2 activity

ART activity in intact Bac1.2F5 macrophages, RAW264.7 macrophages, or BW5147 T lymphocytes was assayed using a western blot protocol based on the 1G4 monoclonal antibody as previously described (36). Briefly, intact cells were transferred to basic salt solution (BSS) containing 130 mM NaCl, 5 mM KCl, 1.5 mM $CaCl_2$, 1 mM $MgCl_2$, 25 mM HEPES (pH 7.5), 5 mM Glucose, and 0.1% BSA. The cells were incubated at 37°C for 15 min with 50 μM ε-NAD and 1 mM ADP-ribose in the presence of 1 mM DTT prior to extraction, SDS-PAGE, and western blotting.

Labeling and immunoprecipitation of ADP-ribosylated P2X7R

HEK293 cells were harvested by trypsinization at 20 h post-co-transfection with P2X7R and either ART2.1 or ART2.2. ART2/P2X7R-coexpressing HEK cells were then incubated at 37° C for 15 min with 50 μM ^{32}P-NAD and 1 mM ADP-ribose in the presence or absence of 1 mM DTT. Washed cells were lysed in PBS, 1% Triton-X100, 1 mM AEBSF (Sigma-Aldrich Corp., St. Louis, MO, USA) for 20 min at 4°C. Insoluble material was pelleted by high-speed centrifugation (15 min, 13,000 *g*). 3 μg/ml K1G Ab (39) was added into the lysate and incubated 2 hours at 4°C, and lysates were further incubated with protein-G Sepharose beads (20 μl beads/lysates from 10^6 cells) for 60 min at 4°C. Immunoprecipitates were washed 3 times using TX-100 buffer. The final product was eluted into 30 μl 2x SDS binding buffer and boiled for 5 min. The samples were loaded on 15% SDS-PAGE gels and proteins were detected by autoradiography. P2X7 was detected with rabbit anti-P2X7 C-terminal peptide antibody (1:1000) (Alomone, Jerusalem, Israel) and peroxidase-conjugated anti-rabbit IgG (1:5000) using the ECL system (Amersham GE-Healthcare, Munich, Germany).

Fluorescence-activated cell sorting analysis

Staining for the P2X7R was performed with Alexa488-conjugated K1G Ab for 30 min at 4°C (39). Stained cells were washed and analyzed on a FACS-Calibur using the Cellquest software (Becton Dickinson). Gating was performed on living cells on the basis of propidium iodide exclusion.

Measurement of P2X7R-mediated Ca^{2+} influx or nucleotide-induced Ca^{2+} mobilization

Macrophages (primary BMDM or macrophage cell lines) were collected into DMEM by gently scraping the monolayers and transferring the detached cells into 50 ml tubes. HEK293 cells were detached by trypsinization. The detached macrophages or HEK293 cells were centrifuged and the cell pellets washed twice with BSS. Primary spleen lymphocytes or BW5147 T cell suspensions were directly pelleted from growth medium prior to washing. Washed cells were resuspended in BSS supplemented with 1 μM fura2-AM and incubated at 37 oC for 40 minutes. The fura2-loaded cells were then washed, resuspended in BSS (10^6/ml), and then stored on ice for up to 3 hours during measurements. For each measurement, a 1.5 ml aliquot of cell suspension was stirred at 37 oC in a quartz cuvette for measurement of fura2-AM fluorescence (339 nm excitation/500 nm emission) and calibration as previously described (40). Murine macrophages (41,42) and HEK293 cells (43,44) also express several subtypes of G protein-coupled, Ca^{2+}-mobilizing P2Y receptors. Thus, the macrophages or HEK293 cells were first treated with a cocktail of 50 μM ADP and 50 μM UTP to activate and desensitize these P2Y receptors prior to P2X7R stimulation by the indicated concentrations of ATP or NAD (45). In some experiments, P2Y receptor-dependent Ca^{2+} mobilization in Bac1.2F5 macrophages or BW5147 T lymphocytes was directly assayed by stimulating the cells with 30 μM ADP, UTP, or UDP. Where indicated, the macrophages or HEK293 cells were treated in the presence or absence of 1 mM DTT (plus 1 mM ADP-ribose, ADP-R) for 1–5 min prior to stimulation with 10–100 μM NAD.

Measurement of P2X7R-mediated YO-PRO-1 or ethidium dye uptake

HEK293 cells transfected with ART2.1 and the hyper-responsive R276K P2X7R variant (21) were gently trypsinated, incubated in the absence or presence of NAD or ATP in 10 mM Hepes pH 7.5, 140 mM NaCl, 5 mM KCl, 10 mM glucose and 1 μM YO-PRO-1 (Molecular Probes) for 60 min at 37°C. Cells were subsequently washed, resuspended in Annexin V binding buffer (BD Biosciences), and stained with Annexin V-APC (BD Biosciences) prior to analysis by flow cytometry. Spleen cells from BALB/c or NZW mice were incubated with YO-PRO-1 as described above, and stained with antibodies against surface markers CD3, B220, and analyzed by flow cytometry. Cells staining positive for CD3 were analyzed for the expression of P2X7R, ART2.1, ART2.2, and the uptake of YO-PRO-1. Control or IFN-γ-primed Bac1.2F5 macrophages were collected in DMEM by gently scraping the monolayers and transfer into 50 ml tubes. The cells were centrifuged, washed and resuspended in BSS. 1.5 ml aliquots of cell suspension were transferred to the stirred measuring cuvette and pre-incubated for 3 min at 37°C. Ethidium bromide (2.5 μM) was added and baseline fluorescence (360 nm excitation/580 nm emission) was recorded prior to stimulation of the cells with various concentrations of NAD and/or ATP as described in the Fig 10 legend. All $ethidium^+$ fluorescence increases were corrected for background dye fluorescence. The P2X7R-mediated increases in $ethidium^+$ accumulation were expressed as a percentage of the maximal fluorescence observed when the cells were permeabilized with 0.003% digitonin.

HPLC analysis of extracellular NAD metabolism

Monolayers of Bac1.2F5 macrophages (10^6 cells/well in 6-well dishes) were incubated in 1 ml BSS at 37°C supplemented with 100 μM NAD in the presence or absence of 1 mM ADP-ribose. At selected times (0–60 min), 100 μl aliquots of the extracellular medium were removed, boiled for 5 min, and centrifuged to sediment any precipitated protein. NAD and its principle metabolite ADP-ribose were separated and quantified using a reverse-phase HPLC protocol. Briefly, 50μl aliquots were injected onto an Alltech C18 Adsorbospherecolumn which was isocratically eluted at 1.3 ml/min with a running buffer of 0.1 M KH_2PO_4/5% methanol/pH 6. NAD (elution time 8.2 min) and ADP-ribose (elution time 4 min) were detected by absorbance at 254 nm.

Statistics

All experiments were repeated 2–6 times using different preparations of primary leukocytes isolated from different mice or with leukocyte cell lines from separate cultures. All data, unless otherwise stated, represent mean±SEM. A 2-tailed, 1-variable Student's t-test was used to analyze these data with statistical significance defined as $p<0.05$.

Results

NAD induces activation of P2X7R in murine lymphocytes but not murine macrophages

We confirmed the ability of extracellular NAD to induce P2X7R activation (as assayed by Ca^{2+} influx) in freshly isolated splenic lymphocytes from BALB/c or C57BL/6 mice (Fig 1A–1B), but not in lymphocytes from P2X7−/− mice (Fig 1C). (Although splenic lymphocytes include both T cells and B cells, P2X7R is not expressed by murine B cells (46)). We tested lymphocytes from the BALB/c and C57BL/6 mouse strains because they express polymorphic variants of the P2X7R (P451 for BALB/c and L451 for C57BL/6) (47). Additionally, T lymphocytes from BALB/c mice express both ART2.1 and ART2.2 as functional enzymes while leukocytes from C57BL/6 mice express only ART2.2 due to a premature stop codon in ART2.1 mRNA that prevents translation of functional protein (34, 35).

In contrast to its actions on T cells, NAD did not trigger Ca^{2+} influx in naive bone marrow-derived macrophages (BMDM) isolated from either BALB/c or C57BL/6 mice (Fig 1D–1E) even though ATP stimulated robust increases in Ca^{2+} in both wildtype BMDM populations, but not in BMDMs from P2X7R-deficient mice (Fig. 1F). This absence of an NAD effect in naive macrophages was consistent with our previous findings that murine macrophages express only low levels of ecto-ARTs in the absence of pro-inflammatory activation by IFNs or LPS. Likewise, C57BL/6 BMDM were unresponsive to NAD even after pro-inflammatory activation by LPS (Fig 1H) or IFNs (not shown); this is consistent with the general lack of ART2.2 expression in murine myeloid leukocytes and the specific lack of ART2.1 expression in C57BL/6 myeloid leukocytes (35). As expected, neither NAD nor ATP elicited a Ca^{2+} influx response in P2X7-knockout BMDM (Fig. 1I). Surprisingly, however, inflammatory BALB/c BMDM, primed with IFNγ (Fig 1G) to up-regulate ART2.1, were also unresponsive to extracellular NAD but retained a robust response to ATP. We have previously described the use of anti-ART2.1, anti-ART2.2, and anti-εADP-ribose mAbs in FACS analyses to confirm that LPS and IFN-γ induced the specific up-regulation of ART2.1 protein and ADP-ribosyltransferase activity in BMDM from wildtype BALB/c mice (36) but not in BMDM from an ART2.1 knockout BALB/c strain (data not shown). Consistent with the thiol-dependence of ART2.1 enzyme activity, inclusion of dithiothreitol (DTT) markedly increases ADP-ribosylation of cell surface proteins in intact BALB/c BMDM (36). However, inclusion of extracellular DTT did not facilitate NAD-induced Ca^{2+} influx in these IFN-primed BMDM (Fig 1G).

The murine P2X7R is a substrate for ADP-ribosylation and gating by the thiol-sensitive ART2.1 ecto-enzyme

The ability of extracellular NAD to activate the P2X7R in BALB/c T cells that express ART2.1 and ART2.2, but not in BALB/c macrophages that express only ART2.1 raised the critical question of whether ART2.1 (similarly to ART2.2) can recognize the P2X7R as a substrate. To test this, the murine P2X7R was co-expressed with ART2.1 or ART2.2 in HEK293 cells. The ART2-expressing cells were briefly incubated with [^{32}P]-NAD in the presence or absence of DTT, prior to extraction, immunoprecipitation of the P2X7R, SDS-PAGE, and detection of [^{32}P]-ADP-ribosylated P2X7R by autoradiography. Fig 2A illustrates the extracellular domain of the murine P2X7R including the relative positions of seven (of the total eighteen) arginine residues within this domain. Previous studies identified R125 and R133 as the critical sites for

ART2.2-catalyzed ADP-ribosylation of the P2X7R (21). Thus, we compared wildtype (WT) P2X7R versus a P2X7R construct (R125KR133K), wherein the two target arginines for ART2.2 within the cysteine-rich loop were replaced by lysine, and which thus could not function as an acceptor for ADP-ribosylation by ART2.2. The expression of ART2.1 in HEK293 cells facilitated the robust ADP-ribosylation of the WT P2X7R but not the double arginine mutant variant as assayed by incorporation of [^{32}P]-ADP-ribose (Fig. 2B). Notably, the ability of ART2.1 to ADP-ribosylate the wildtype P2X7R was highly dependent on exogenously added DTT. In contrast, HEK293 cells co-expressing ART2.2 and wildtype P2X7R showed strong and equivalent [^{32}P]-ADP-ribosylation of P2X7R the absence or presence of DTT; mutants of P2X7 in which the R125 and R133 residues were changed to lysine did not function as a substrate for ART2.2 regardless of the presence or absence of DTT (data not shown). Importantly, we used the K1G anti-P2X7 antibody and FACS analyses to confirm similar cell surface expression levels of all wildtype and mutant P2X7R constructs (Fig 2).

We next asked whether ADP-ribosylation of P2X7R by ART2.1 also induces the gating of P2X7R. To this end, we examined NAD-induced and P2XR7-dependent pore formation in T lymphocytes from BALB/c mice, which express both ART2.1 and ART2.2 or corresponding cells from NZW mice, which lack ART2.2 and express only ART2.1 (Fig 2C). The formation of membrane pores that allow the incorporation of DNA-staining dyes like YO-PRO-1 is considered to be a typical hallmark of P2X7 activation. Figure 2D shows that T lymphocytes from BALB/c mice, which express high levels of ART2.2, incorporate YO-PRO-1 in response to micromolar NAD, regardless of the presence or absence of DTT. In contrast, NAD-induced YO-PRO-1 uptake into T lymphocytes from NZW mice, which express only ART2.1, is strictly dependent on DTT and also requires higher concentrations of NAD.

NAD potentiates ATP-induced P2X7R activation in HEK293 cells co-expressing ART2 and P2X7R

The data in Fig 2 verified the ability of NAD to effectively ADP-ribosylate the wildtype murine P2X7R when heterologously expressed with ART2.1 in the HEK293 cell background. However, we have reported that this covalent modification of the wildtype P2X7R expressed in HEK293 cells is not sufficient for functional activation of the receptor (21). Fig. 3A shows this by comparing NAD versus ATP as stimuli for Ca^{2+} influx in an HEK293 line (HEK-mP2X7 cells) stably transfected with murine P2X7R cDNA prior to transient transfection with an ART2.2 expression plasmid. Western blot analysis confirmed the expression of functional ART activity in ART2.2-transfected, but not parental, HEK293 cells (Fig 3C). This assay involves incubation of intact cells with εNAD (an NAD analog) to covalently ε-ADP-ribosylate cell surface proteins followed by cell extraction, SDS-PAGE, and probing with the anti-ε-ADP-ribose 1G4 mAb. Fig 3C also shows that inclusion of extracellular ADP-ribose (ADP-R) potentiated accumulation of ADP-ribosylated proteins by attenuating the metabolism of eNAD (or NAD) by ecto-nucleotidases. Despite the robust ART activity in the co-transfected HEK-mP2X7 cells, extracellular NAD did not mimic the ability of ATP to trigger P2X7R-dependent Ca^{2+} influx.

We have described another P2X7R arginine residue (R276), which is not an ecto-ADP-ribosylation site, but is a critical modulator of ATP potency (21). Fig 3B shows that HEK293 line (HEK-mP2X7-R276K), stably transfected with the R276K gain of function mutant of P2X7R, exhibited a maximal Ca^{2+} influx response to 50 μM ATP which is a sub-threshold concentration in cells expressing wildtype P2X7R (Fig. 4A). Notably, this R276K mutation also facilitated the gating of P2X7R channel activity in response to NAD in HEK293 cells co-transfected with ART2.2 (Fig. 3B).

Fig 3D demonstrates that ART2.1 also mediates the NAD-dependent activation of the hypersensitive R276K-mutant P2X7R in transiently co-transfected HEK293 cells. These experiments utilized two FACS-based readouts of P2X7R function: 1) the transfer of phosphatidylserine to the external leaflet of the plasma membrane bilayer ("PS-flip") as measured by increased binding of fluorochrome-conjugated Annexin V; and 2) induction of the non-selective permeability pore as measured by influx of YO-PRO-1 dye. In the absence of either ATP or NAD stimuli, the cells exhibited little if any surface Annexin V staining or YO-PRO-1 accumulation. When stimulated by ATP, the majority of the ART2.1-mP2X7-R276K co-transfected HEK cells showed strongly increased Annexin V binding and YO-PRO-1 uptake. Treatment with NAD in the presence of DTT caused a similar stimulation of Annexin V binding but a somewhat lower induction of YO-PRO-1 uptake. In contrast, cells treated with ADP-R plus DTT exhibited control levels of annexin binding and dye accumulation. Notably, these PS-flip and YO-PRO-1 influx responses to NAD were absent when the R276K mutation was combined with the double R125K133K substitutions that eliminate the P2X7 ADP-ribosylation sites targeted by ART2.1. In contrast, and in accord with our previous report (21), the triple R276K125K133K mutant of P2X7 retained robust responses to ATP.

The differential ability of NAD/ART2 to activate the R276K-mutated P2X7R (Figs. 3B and 3D), but not the wildtype P2X7R (Fig. 3A), in an HEK293 background is similar to the observations in Fig. 1 regarding the differential ability of NAD to activate P2X7R in murine T lymphocytes, but not in murine macrophages. These differences indicate that the consequences of ADP-ribosylation on P2X7R function are cell-type specific, perhaps due to the differential expression of cell-specific accessory signaling molecules or of variant forms of P2X7R. We tested the hypothesis that ADP-ribosylation of wildtype P2X7R in HEK293 cells, while insufficient to activate the receptor per se, might modulate the ATP activation threshold. HEK293 cells co-expressing ART2.2 and wildtype P2X7R were pre-stimulated with or without 100 μM NAD for 3–5 min prior to being challenged with increasing concentrations of ATP to activate P2X7R-mediated Ca^{2+} influx. The NAD pretreatment decreased the threshold concentration of ATP required to stimulate P2X7R in cells that co-expressed ART2 (Figs 4A and 4B). Figs. 4C–4F compare the quantification of ATP-induced changes in Ca^{2+} (+/− NAD pretreatment) at 30 s (Figs 4C and 4E) and 3 min (Figs 4D and 4F) in ART2-transfected or non-transfected HEK-mP2X7 cells. The NAD-induced shift in ATP sensitivity was most apparent with [ATP] in the 200–600 μM range. NAD did not further increase the Ca^{2+} influx response to [ATP]≥1mM which maximally activates P2X7R function. Notably, NAD pretreatment did not shift the ATP dose-response relationship in the HEK293 cells expressing P2X7R but not ART2.2 (Figs 4B, 4E, and 4F).

These experiments focused on defining changes in P2X7R activation by [ATP] in the threshold-to-EC_{50} range because we (16) and others (2,15) have noted that conventional analysis of ATP concentration-response relationships for recombinant or native P2X7R is complicated by: 1) the unusually high ATP EC_{50} (~1 mM), 2) the allosteric effects of extracellular Mg^{2+} and Ca^{2+} on P2X7R activity, and 3) the strong chelation of divalent cations by ATP (a divalent anion at physiological pH and ionic strength) such that extracellular concentrations of free Mg^{2+} and free Ca^{2+} are decreased as the concentration of added ATP is increased to supramillimolar levels. The assay of Ca^{2+} influx as a sensitive and convenient readout of P2X7R channel gating is further convoluted by the decreased extracellular [Ca^{2+}] and consequent reduction in chemical driving force at supramillimolar [ATP]. Because, the contribution of these various complicating factors is minimized at submillimolar [ATP], we assayed changes in threshold ATP concentrations rather than changes in the ATP EC50 as the simplest index of increased ATP potency at ADP-ribosylated P2X7R.

Differential effects of NAD/ART2 on P2X7R function in established murine macrophage and T lymphocyte cell lines

That NAD treatment decreased the threshold ATP concentration for heterologously expressed P2X7R in HEK293 suggested that NAD/ART2.1 might similarly regulate natively expressed P2X7R in murine macrophages. To facilitate these studies, we first determined that established murine macrophage and T cell lines were appropriate models for mechanistic analysis of the differential effects of NAD/ART2 on P2X7R function in primary murine macrophages versus T cells. We tested two murine macrophage cell lines (Bac1.2F5 and RAW264.7) and a murine T lymphoma cell line (BW5147). As in primary BMDM (36), the Bac1.2F5 macrophages (Fig 5A) and RAW264.7 macrophages (data not shown) lacked basal expression of any ecto-ART subtypes at the mRNA level. (Heart or spleen extracts from BALB/c mice were used as positive control sources of ART 1, 2, 3, 4, and 5 transcripts). However, Bac1.2F5 cells stimulated with 100 ng/ml LPS for 2 – 24 hr selectively accumulated ART2.1 mRNA (Fig 5C) and this up-regulation of ART2.1 was correlated with increased expression of iNOS and IFN-β, two other LPS-inducible gene products. Thiol-dependent ART enzyme activity in intact Bac1.2F5 macrophages was detected using the 1G4 mAb-based Western blot assay (Fig 5D). Multiple cell surface proteins were ADP-ribosylated, in a strictly DTT-dependent manner, in Bac1.2F5 macrophages primed by LPS, IFN-γ, or IFN-β to up-regulate ART2.1 expression (Fig. 5D). Extracellular GSH, a physiological thiol reductant, also supported the ADP-ribosylation of multiple surface proteins in the IFN-primed macrophages (Fig 5E). Similar to primary spleen T cells from BALB/c mice, BW5147 T lymphoma cells constitutively expressed both ART2.1 and ART2.2 mRNA (Fig 5A and 5B) and also expressed functional ART2 activity as detected by the 1G4 mAb assay (data not shown). Splenic T cells from C57BL/6 mice expressed ART2.2 but not ART2.1 at significant levels. Notably, the BW5147 T cells also exhibited robust Ca^{2+} influx responses to either ATP or NAD (Fig 5F) as observed in primary splenic lymphocytes (Figs 1A and 1B). In contrast, IFN-γ-primed Bac1.2F5 macrophages responded to exogenous ATP, but not to NAD alone (Fig 5G), similar to IFN- or LPS-primed primary BMDM (Fig 1D).

Recent studies have indicated that extracellular NAD also activates some subtypes of G protein-coupled P2Y nucleotide receptors that can trigger mobilization of intracellular Ca^{2+} stores (48). The Ca^{2+} influx-based assay used to monitor P2X7R activity required prestimulation of the macrophages with a cocktail of ADP and UTP to first activate and desensitize the Ca^{2+}-mobilizing P2Y1, P2Y2, and P2Y6 receptors expressed in these cells (41,42). We tested the possibility that this protocol also desensitized NAD-reactive P2Y receptors that might be expressed in T cells and macrophages. BW5147 and Bac1.2F5 macrophages were stimulated with only single nucleotide agonists with no prior desensitization incubation. Although murine T cells have been reported to express mRNA for various P2Y receptor subtypes(14), we observed no Ca^{2+}-mobilizing responses to micromolar concentrations of ADP (P2Y1 agonist), UTP (P2Y2/P2Y4 agonist), or UDP (P2Y6 agonist) in the BW5147 T cells (Fig. 6A). Moreover, primary T cells from P2X7R-knockout mice showed no Ca^{2+} response to ATP or NAD (Fig 1). Thus, naive murine T cells do not express functionally significant levels of Ca^{2+}-mobilizing P2Y receptors that can be activated by ATP, ADP, UTP, UDP, or NAD. In contrast, Bac1 macrophages – like primary murine BMDM (36) – exhibited strong Ca^{2+} mobilization responses to ADP, UTP, and UDP, but not to NAD (Fig 6B). Thus, the differential responses of T cells versus macrophages to NAD do not involve obvious roles for NAD-sensitive P2Y receptor subtypes.

Other ecto-enzymes that modulate the efficiency of NAD-dependent ADP-ribosylation of cell surface proteins can also be differentially expressed in leukocyte subsets. These include the CD38 NAD-glycohydrolases and CD203 nucleotide pyrophosphatases that metabolize extracellular NAD and thereby reduce substrate drive to the ARTs (26). We used HPLC

analyses to test whether the inability of NAD per se to trigger Ca^{2+} influx or mobilization in murine macrophages was due to very rapid metabolism of the added extracellular NAD. Although Bac1 macrophages metabolized 100 μM NAD to ADP-ribose, the $t_{1/2}$ for this reaction was ~20 min such that >50 μM NAD was present throughout the 1–10 min test periods used to assay Ca^{2+} influx/mobilization responses (Fig 6C). Inclusion of exogenous ADP-ribose (routinely added to maintain ADP-ribosylation of target proteins) further slowed the rate of NAD clearance. Thus, excessive NAD catabolism is an unlikely reason for the differential responses or macrophages versus T cells to extracellar NAD.

NAD potentiates ATP-induced P2X7R activation in murine macrophages and T lymphocytes

IFN-γ-primed Bac1.2F5 macrophages were briefly pretreated with NAD in the presence of DTT to allow ADP-ribosylation of cell surface proteins, and then challenged with various doses of ATP to trigger P2X7R-dependent Ca^{2+} influx. Similar to its effects in ART2/P2X7-transfected HEK293 cells, NAD pretreatment increased the sensitivity of the IFN-primed Bac1 macrophages to submillimolar ATP (Figs. 7A–C). In contrast, naive Bac1.2F5 cells, which were not primed with IFN-γ and thus lack expression of ART2.1, did not exhibit the NAD-dependent increase in ATP sensitivity (Figs 7D and 7E). Additional experiments demonstrated that NAD pretreatment produced similar increases in ATP sensitivity in other murine macrophage models including IFN-β-primed RAW264.7 macrophages (Fig. 8A) and IFN-γ-primed BALB/c primary BMDM (Fig 8B). Similar to Bac1.2F cells (Fig 5) and primary BMDM (36), the RAW264.7 macrophage line exhibited upregulation of ART2.1 mRNA and thiol-dependent ecto-ART activity in response to IFN-β stimulation (data not shown).

NAD pretreatment also increased the sensitivity to ATP in the BW5147 T lymphocytes. These experiments involved stimulation of these cells with submaximally active concentrations of NAD (10 μM) and/or ATP (300 μM). Notably, when combined, 10 μM NAD and 300 μM ATP acted synergistically to increase P2X7R-mediated Ca^{2+} influx (Fig. 8C).

ART2 can utilize dinucleotide substrates other than NAD to covalently ribosylate arginine residues in target proteins; these alternative substrates include ε-NAD and NGD (nicotinamide guanine dinucleotide). We previously reported that ribosylation of the P2X7R byε-NAD or NGD in primary murine T cells does not stimulate the receptor but rather antagonizes NAD-induced receptor activation (20). We observed similar effects of ε-NAD on P2X7R function in the BW5147 T cell line (Figs. 9A and 9B). Notably, P2X7 receptors ribosylated byεNAD also have decreased sensitivity to activation by submaximal ATP as shown in primary murine T cells (20), BW5147 T lymphoma cells (Figs 9A and 9B), IFN-γ-primed Bac1.2F5 macrophages (Fig. 9C), and IFN-β-primed RAW264.7 macrophages (Fig 9D).

NAD potentiates ATP-induced P2X7R-dependent pore formation in murine macrophages

The previous data showing that ADP-ribosylation of P2X7R potentiates ATP activation of these receptors in murine macrophages and HEK293 cells used increases in cytosolic Ca^{2+} as a sensitive readout of P2X7R channel activity. We considered the possibility that the P2Y prestimulation protocol (used to desensitize Ca^{2+}-mobilizing P2Y receptors) triggered G protein-coupled signaling pathways that modulate the functional interactions between ART2 and P2X7R in macrophages and HEK293 cells. Thus, we measured the effects of NAD/ART2 on non-selective pore formation as an alternative readout of P2X7R activation that does not require prestimulation and desensitization of P2Y receptors. Pore formation was assayed by ethidium accumulation in IFN-γ-primed (Fig 10A) versus control (Fig 10B) Bac1.2F5 macrophages, similar to the YO-PRO-1 accumulation assay previously described for HEK293 cells (Fig 3D). NAD (plus DTT) by itself did not stimulate ethidium accumulation but did increase the rate of accumulation triggered by submillimolar ATP in the IFN-γ primed but not control Bac1 macrophages. Notably, the potentiating effects of NAD on ethidium influx were

observed at a higher range of extracellular ATP concentrations (0.5 –1 mM) than the effects on Ca^{2+} influx (0.1 – 0.5 mM ATP; Fig 7). This is consistent with the fact that ethidium influx is a secondary response to P2X7R stimulation (49) that involves gating of pannexin-1 hemichannels (4). Previous studies have indicated that the ATP concentration-response relationship describing this secondary response is right-shifted relative to the concentration-response relationship describing the primary gating of P2X7R channels (2,50).

Discussion

From the initial functional characterization of the permeabilizing "P2Z" ATP receptor 30 years ago (51–53), through the molecular identification of the P2Z receptor phenotype as the product of the P2X7R gene (2), and up to the most recent analyses of *in vivo* functional deficits in P2X7-knockout mice (10,11,54), two fundamental and perplexing questions regarding the P2X7R have been repeatedly considered. First, why does this particular ATP receptor, in sharp contrast to the six other P2X receptor subtypes, require millimolar levels of extracellular ATP for activation when studied in isolated cells? This unusual characteristic suggests that low affinity variants of an ancestral P2X7R were favored by positive selection as the receptor acquired its physiological roles as a regulator of proinflammatory signaling and cell death. Low ATP affinity prevents inadvertent activation of these highly consequential but poorly reversible responses until leukocytes accumulate at sites of tissue damage or microbial invasion. However, this raises a second and corollary question: how does the P2X7R become activated in leukocytes within these latter tissue compartments given the receptor's low affinity of ATP? Recent studies support three possible mechanisms that are not mutually exclusive: 1) highly localized accumulation of ATP for autocrine activation of P2X7R within diffusion-restricted cell surface compartments (13,14,55); 2) allosteric modulation of ATP affinity via conformational changes in P2X7 trimeric channels produced by local biophysical conditions or covalent modification of the P2X7R protein itself (15,16,18,19,56,57); and 3) the ATP-independent activation of P2X7R via conformational changes produced by ADP-ribosylation of key arginines within the extracellular loop of the P2X7R (20,21,58). The experiments described in this report provide new insights into the latter two regulatory mechanisms and additionally suggest that a fourth mechanism – involving tissue/cell-selective expression of accessory molecules and/or of P2X7R splice variants – contribute to the regulation of P2X7R function.

The ability of NAD to drive the covalent modification of extracellular residues of the P2X7R comprises a novel mechanism to produce relatively long-lasting changes in the conformational state of these ligand-gated ion channels during transient increases in extracellular NAD, ATP, and other normally intracellular metabolites, such as lyso-lipids, that can regulate P2X7R function (22,58,59). Previous studies demonstrated that NAD can trigger P2X7R activation in murine T lymphocytes even when these cells were incubated in the presence of apyrase to scavenge any released ATP (20). Moreover, P2X7R activation was sustained in T cells briefly treated with NAD and then washed free of this nucleotide. In contrast, ATP-stimulated P2X7R rapidly deactivated when T cells were transferred to ATP-free medium. These findings indicate that ADP-ribosylation of P2X7R subunits in murine T cells induces a conformational change sufficient to gate the opening of these trimeric channels even in absence of ATP binding. However, our studies of P2X7R function in murine macrophages and HEK293 cells indicate that this ATP-independent activation of P2X7R by ADP-ribosylation is not a general mode of P2X7R regulation but rather reflects specialized conditions present in murine T lymphocytes.

Notably, while NAD by itself was able to gate P2X7R in NZW T lymphocytes expressing solely ART2.1, it failed to activate P2X7R either in murine macrophages that co-express native P2XR7 and ART2.1 or in HEK293 cells engineered to co-express murine P2X7R and murine ART2 ecto-enzymes. However, NAD acted synergistically with ATP to regulate P2X7R in

both the macrophages and the engineered HEK cells, and this effect of NAD was strictly dependent on the expression of ART2.1 or ART2.2 in both cell models. How can these regulatory effects of NAD/ART2 on ATP-dependent P2X7R activation observed in murine macrophages and HEK293 cells be reconciled with the robust ATP-independent activation by NAD/ART2 in murine T cells? A possible explanations for the difference in P2X7R signaling observed between myeloid and lymphoid cells are that T cells, but not macrophages or HEK cells, express other regulatory proteins that facilitate the ATP-independent gating of P2X7R in response to ADP-ribosylation, or that the local membrane microenvironments containing P2X7R and ART2 are different in the two cell types. Another possible explanation might be the expression of different recently identified splice variants of rodent P2X7R in T cells versus macrophages. Indeed, Taylor et al. have recently reported that P2X7 receptor function is preserved in the T lymphocytes, but not macrophages, from one strain of P2X7-null mice which was generated by lacZ insertion into exon 1 of the *p2rx7* gene (60). Determining whether different murine tissues, particularly hematopoietic cells, differentially express splice variants of the P2X7R with altered functional responses to ART2-mediated modification is an important goal for future experiments.

It is important to consider how ADP-ribosylation of key Arg residues may affect the conformation of these trimeric channels. Electrophysiological analyses of P2X-family channels, at the whole cell and single-channel levels, indicate that at least 2, and probably 3, molecules of ATP need to be bound per channel for optimal gating (9,61). Moreover, the critical ATP binding sites appear to be formed at the interfaces between the extracellular loops of individual subunits, rather than within each subunit loop as initially hypothesized (62,63). In this regard, the covalently associated ADP-ribose at Arg-125 of a P2X7 subunit may interact with the key interfacial amino residues that form the ATP-binding site. However, ADP-ribose is larger than ATP per se and it is unclear whether the P2X7R channel complex can accommodate ADP-ribosylation of all 3 subunits or whether only 1 or 2 subunits per channel can be efficiently modified. Differences in the number of covalently modified subunits per channel, due possibly to steric hindrance, may underlie the distinctive consequences of NAD/ART2 action on P2X7R function in macrophages versus T cells. ADP-ribosylation of these receptors in macrophages may be limited to only 1 or 2 subunits per channel, which is insufficient for gating but sufficient for positive allosteric action at the remaining interfacial ATP binding sites. This would be consistent with the observed increase in potency of ATP at P2X7R in ART2.1 expressing macrophages (or HEK293 cells) pretreated with NAD. In contrast, the predominant P2X7R channels in T cells, or the mutant P2X7R-R276K channels in HEK cells, may have conformations that accommodate permit ADP-ribosylation of all 3 subunits.

It is currently unclear whether ADP-ribosylation is a common mechanism for the activation or sensitization of P2X7R signaling in other tissues or organisms. Notably, the Arg-125 and Arg-133 residues are conserved in the human P2X7R (64), but the human ART2A and ART2B are transcriptionally silent pseudo-genes (26,65). Thus, human T cells and macrophages lack the capacity for *cis*-regulation of P2X7R by a co-expressed ecto-ART. However, human ART1 is constitutively expressed in neutrophils and this GPI-anchored enzyme is rapidly shed during neutrophil activation in response to bacterial infection (66). ART1 is also expressed by human airway epithelial cells basally and at increased levels in response to bacterial mediators (67–69). Thus, the P2X7R in human macrophages and T cells might be *trans*-regulated by shed ART1 that accumulates at sites of bacterial infection and neutrophil recruitment. Such a mechanism may also be operative in mice which also express ART1 in other tissues such as cardiac and skeletal muscle (70).

NAD is released to extracellular environments during the early stage of inflammatory response (58). Besides its ability to trigger P2X7R-dependent T cell death (20), extracellular NAD has

been reported as an agonist for P2Y11 receptors in human granulocytes (48). Our study now shows that NAD also increases the sensitivity of the P2X7R to ATP gating in macrophages. This action of NAD requires expression of the thiol-sensitive ART2.1 enzymes and reduced thiols, such as glutathione and cysteine, that can accumulate at inflammatory loci due to release from activated macrophages and the hypoxia that often characterizes such loci (31). We have found that ART2.1 is widely expressed in other leukocytes, such as dendritic cells and B lymphocytes (71). Thus, the sensitization of ATP-dependent P2X7R activation by NAD/ART2.1 may provide an additional layer of regulatory control in multiple phases of innate and adaptive immunity.

References

1. North RA. Molecular physiology of P2X receptors. Physiol Rev 2002;82:1013–1067. [PubMed: 12270951]
2. Surprenant A, Rassendren F, Kawashima E, North RA, Buell G. The cytolytic P2Z receptor for extracellular ATP identified as a P2X receptor (P2X7). Science 1996;272:735–738. [PubMed: 8614837]
3. Nicke A. Homotrimeric complexes are the dominant assembly state of native P2X7 subunits. Biochem Biophys Res Commun 2008;377:803–808. [PubMed: 18938136]
4. Pelegrin P, Surprenant A. Pannexin-1 mediates large pore formation and interleukin-1beta release by the ATP-gated P2X7 receptor. EMBO J 2006;25:5071–5082. [PubMed: 17036048]
5. Lister MF, Sharkey J, Sawatzky DA, Hodgkiss JP, Davidson DJ, Rossi AG, Finlayson K. The role of the purinergic P2X7 receptor in inflammation. J Inflamm (Lond) 2007;4:5. [PubMed: 17367517]
6. Ferrari D, Pizzirani C, Adinolfi E, Lemoli RM, Curti A, Idzko M, Panther E, Di Virgilio F. The P2X7 receptor: a key player in IL-1 processing and release. J Immunol 2006;176:3877–3883. [PubMed: 16547218]
7. Di Virgilio F, Wiley JS. The P2X7 receptor of CLL lymphocytes-a molecule with a split personality. Lancet 2002;360:1898–1899. [PubMed: 12493250]
8. Dubyak GR. Go it alone no more--P2X7 joins the society of heteromeric ATP-gated receptor channels. Mol Pharmacol 2007;72:1402–1405. [PubMed: 17895406]
9. Khakh BS, North RA. P2X receptors as cell-surface ATP sensors in health and disease. Nature 2006;442:527–532. [PubMed: 16885977]
10. Chessell IP, Hatcher JP, Bountra C, Michel AD, Hughes JP, Green P, Egerton J, Murfin M, Richardson J, Peck WL, Grahames CB, Casula MA, Yiangou Y, Birch R, Anand P, Buell GN. Disruption of the P2X7 purinoceptor gene abolishes chronic inflammatory and neuropathic pain. Pain 2005;114:386–396. [PubMed: 15777864]
11. Ke HZ, Qi H, Weidema AF, Zhang Q, Panupinthu N, Crawford DT, Grasser WA, Paralkar VM, Li M, Audoly LP, Gabel CA, Jee WS, Dixon SJ, Sims SM, Thompson DD. Deletion of the P2X7 nucleotide receptor reveals its regulatory roles in bone formation and resorption. Mol Endocrinol 2003;17:1356–1367. [PubMed: 12677010]
12. Netea MG, Nold-Petry CA, Nold MF, Joosten LA, Opitz B, van der Meer JH, van de Veerdonk FL, Ferwerda G, Heinhuis B, Devesa I, Funk CJ, Mason RJ, Kullberg BJ, Rubartelli A, van der Meer JW, Dinarello CA. Differential requirement for the activation of the inflammasome for processing and release of IL-1beta in monocytes and macrophages. Blood 2009;113:2324–2335. [PubMed: 19104081]
13. Piccini A, Carta S, Tassi S, Lasiglie D, Fossati G, Rubartelli A. ATP is released by monocytes stimulated with pathogen-sensing receptor ligands and induces IL-1beta and IL-18 secretion in an autocrine way. Proc Natl Acad Sci U S A 2008;105:8067–8072. [PubMed: 18523012]
14. Schenk U, Westendorf AM, Radaelli E, Casati A, Ferro M, Fumagalli M, Verderio C, Buer J, Scanziani E, Grassi F. Purinergic control of T cell activation by ATP released through pannexin-1 hemichannels. Sci Signal 2008;1:ra6. [PubMed: 18827222]
15. Michel AD I, Chessell P, Humphrey PP. Ionic effects on human recombinant P2X7 receptor function. Naunyn Schmiedebergs Arch Pharmacol 1999;359:102–109. [PubMed: 10048594]

16. Verhoef PA, Kertesy SB, Lundberg K, Kahlenberg JM, Dubyak GR. Inhibitory effects of chloride on the activation of caspase-1, IL-1beta secretion, and cytolysis by the P2X7 receptor. J Immunol 2005;175:7623–7634. [PubMed: 16301672]

17. Riedel T, Schmalzing G, Markwardt F. Influence of extracellular monovalent cations on pore and gating properties of P2X7 receptor-operated single-channel currents. Biophys J 2007;93:846–858. [PubMed: 17483156]

18. Michel AD, Fonfria E. Agonist potency at P2X7 receptors is modulated by structurally diverse lipids. Br J Pharmacol 2007;152:523–537. [PubMed: 17700717]

19. Takenouchi T, Iwamaru Y, Sugama S, Sato M, Hashimoto M, Kitani H. Lysophospholipids and ATP mutually suppress maturation and release of IL-1 beta in mouse microglial cells using a Rho-dependent pathway. J Immunol 2008;180:7827–7839. [PubMed: 18523246]

20. Seman M, Adriouch S, Scheuplein F, Krebs C, Freese D, Glowacki G, Deterre P, Haag F, Koch-Nolte F. NAD-induced T cell death: ADP-ribosylation of cell surface proteins by ART2 activates the cytolytic P2X7 purinoceptor. Immunity 2003;19:571–582. [PubMed: 14563321]

21. Adriouch S, Bannas P, Schwarz N, Fliegert R, Guse AH, Seman M, Haag F, Koch-Nolte F. ADP-ribosylation at R125 gates the P2X7 ion channel by presenting a covalent ligand to its nucleotide binding site. FASEB J 2008;22:861–869. [PubMed: 17928361]

22. Haag F, Adriouch S, Brass A, Jung C, Moller S, Scheuplein F, Bannas P, Seman M, Koch-Nolte F. Extracellular NAD and ATP: Partners in immune cell modulation. Purinergic Signal 2007;3:71–81. [PubMed: 18404420]

23. Bortell R, Kanaitsuka T, Stevens LA, Moss J, Mordes JP, Rossini AA, Greiner DL. The RT6 (Art2) family of ADP-ribosyltransferases in rat and mouse. Mol Cell Biochem 1999;193:61–68. [PubMed: 10331639]

24. Sardinha DF, Rajan TV. Cis-acting regulation of splenic Art2 gene expression in inbred mouse strains. Immunogenetics 1999;49:700–703. [PubMed: 10369930]

25. Koch-Nolte F, Duffy T, Nissen M, Kahl S, Killeen N, Ablamunits V, Haag F, Leiter EH. A new monoclonal antibody detects a developmentally regulated mouse ecto-ADP-ribosyltransferase on T cells: subset distribution, inbred strain variation, and modulation upon T cell activation. J Immunol 1999;163:6014–6022. [PubMed: 10570289]

26. Seman M, Adriouch S, Haag F, Koch-Nolte F. Ecto-ADP-ribosyltransferases (ARTs): emerging actors in cell communication and signaling. Curr Med Chem 2004;11:857–872. [PubMed: 15078170]

27. Kawamura H, Sugiyama T, Wu DM, Kobayashi M, Yamanishi S, Katsumura K, Puro DG. ATP: a vasoactive signal in the pericyte-containing microvasculature of the rat retina. J Physiol 2003;551:787–799. [PubMed: 12876212]

28. Aswad F, Kawamura H, Dennert G. High sensitivity of CD4+CD25+ regulatory T cells to extracellular metabolites nicotinamide adenine dinucleotide and ATP: a role for P2X7 receptors. J Immunol 2005;175:3075–3083. [PubMed: 16116196]

29. Hara N, Terashima M, Shimoyama M, Tsuchiya M. Mouse T-cell antigen rt6.1 has thiol-dependent NAD glycohydrolase activity. J Biochem (Tokyo) 2000;128:601–607. [PubMed: 11011142]

30. Yeh MW, Kaul M, Zheng J, Nottet HS, Thylin M, Gendelman HE, Lipton SA. Cytokine-stimulated, but not HIV-infected, human monocyte-derived macrophages produce neurotoxic levels of l -cysteine. J Immunol 2000;164:4265–4270. [PubMed: 10754324]

31. Moriarty-Craige SE, Jones DP. Extracellular thiols and thiol/disulfide redox in metabolism. Annu Rev Nutr 2004;24:481–509. [PubMed: 15189129]

32. Haag F, Freese D, Scheublein F, Ohlrogge W, Adriouch S, Seman M, Koch-Nolte F. T cells of different developmental stages differ in sensitivity to apoptosis induced by extracellular NAD. Dev Immunol 2002;9:197–202. [PubMed: 15144016]

33. Ohlrogge W, Haag F, Lohler J, Seman M, Littman DR, Killeen N, Koch-Nolte F. Generation and characterization of ecto-ADP-ribosyltransferase ART2.1/ART2.2-deficient mice. Mol Cell Biol 2002;22:7535–7542. [PubMed: 12370300]

34. Adriouch S, Ohlrogge W, Haag F, Koch-Nolte F, Seman M. Rapid induction of naive T cell apoptosis by ecto-nicotinamide adenine dinucleotide: requirement for mono(ADP-ribosyl)transferase 2 and a downstream effector. J Immunol 2001;167:196–203. [PubMed: 11418649]

35. Kanaitsuka T, Bortell R, Stevens LA, Moss J, Sardinha D, Rajan TV, Zipris D, Mordes JP, Greiner DL, Rossini AA. Expression in BALB/c and C57BL/6 mice of Rt6–1 and Rt6–2 ADP-ribosyltransferases that differ in enzymatic activity: C57BL/6 Rt6–1 is a natural transferase knockout. J Immunol 1997;159:2741–2749. [PubMed: 9300695]

36. Hong S, Brass A, Seman M, Haag F, Koch-Nolte F, Dubyak GR. Lipopolysaccharide, IFN-gamma, and IFN-beta induce expression of the thiol-sensitive ART2.1 Ecto-ADP-ribosyltransferase in murine macrophages. J Immunol 2007;179:6215–6227. [PubMed: 17947697]

37. Koch-Nolte F, Glowacki G, Bannas P, Braasch F, Dubberke G, Ortolan E, Funaro A, Malavasi F, Haag F. Use of genetic immunization to raise antibodies recognizing toxin-related cell surface ADP-ribosyltransferases in native conformation. Cell Immunol 2005;236:66–71. [PubMed: 16271711]

38. Myers AJ, Eilertson B, Fulton SA, Flynn JL, Canaday DH. The purinergic P2X7 receptor is not required for control of pulmonary Mycobacterium tuberculosis infection. Infect Immun 2005;73:3192–3195. [PubMed: 15845532]

39. Adriouch S, Dubberke G, Diessenbacher P, Rassendren F, Seman M, Haag F, Koch-Nolte F. Probing the expression and function of the P2X7 purinoceptor with antibodies raised by genetic immunization. Cell Immunol 2005;236:72–77. [PubMed: 16165114]

40. Humphreys BD, Virginio C, Surprenant A, Rice J, Dubyak GR. Isoquinolines as antagonists of the P2X7 nucleotide receptor: high selectivity for the human versus rat receptor homologues. Mol Pharmacol 1998;54:22–32. [PubMed: 9658186]

41. del Rey A, Renigunta V, Dalpke AH, Leipziger J, Matos JE, Robaye B, Zuzarte M, Kavelaars A, Hanley PJ. Knock-out mice reveal the contributions of P2Y and P2X receptors to nucleotide-induced Ca2+ signaling in macrophages. J Biol Chem 2006;281:35147–35155. [PubMed: 16980298]

42. da Cruz CM, Ventura AL, Schachter J, Costa-Junior HM, da Silva Souza HA, Gomes FR, Coutinho-Silva R, Ojcius DM, Persechini PM. Activation of ERK1/2 by extracellular nucleotides in macrophages is mediated by multiple P2 receptors independently of P2X7-associated pore or channel formation. Br J Pharmacol 2006;147:324–334. [PubMed: 16341234]

43. Beigi RD, Kertesy SB, Aquilina G, Dubyak GR. Oxidized ATP (oATP) attenuates proinflammatory signaling via P2 receptor-independent mechanisms. Br J Pharmacol 2003;140:507–519. [PubMed: 14522842]

44. Schachter JB, Sromek SM, Nicholas RA, Harden TK. HEK293 human embryonic kidney cells endogenously express the P2Y1 and P2Y2 receptors. Neuropharmacology 1997;36:1181–1187. [PubMed: 9364473]

45. Qu Y, Franchi L, Nunez G, Dubyak GR. Nonclassical IL-1 beta secretion stimulated by P2X7 receptors is dependent on inflammasome activation and correlated with exosome release in murine macrophages. J Immunol 2007;179:1913–1925. [PubMed: 17641058]

46. Elliott JI, Sardini A, Cooper JC, Alexander DR, Davanture S, Chimini G, Higgins CF. Phosphatidylserine exposure in B lymphocytes: a role for lipid packing. Blood 2006;108:1611–1617. [PubMed: 16684961]

47. Adriouch S, Dox C, Welge V, Seman M, Koch-Nolte F, Haag F. Cutting edge: a natural P451L mutation in the cytoplasmic domain impairs the function of the mouse P2X7 receptor. J Immunol 2002;169:4108–4112. [PubMed: 12370338]

48. Moreschi I, Bruzzone S, Nicholas RA, Fruscione F, Sturla L, Benvenuto F, Usai C, Meis S, Kassack MU, Zocchi E, De Flora A. Extracellular NAD+ is an agonist of the human P2Y11 purinergic receptor in human granulocytes. J Biol Chem 2006;281:31419–31429. [PubMed: 16926152]

49. Nuttle LC, Dubyak GR. Differential activation of cation channels and non-selective pores by macrophage P2z purinergic receptors expressed in Xenopus oocytes. J Biol Chem 1994;269:13988–13996. [PubMed: 7514597]

50. Gudipaty L, Humphreys BD, Buell G, Dubyak GR. Regulation of P2X(7) nucleotide receptor function in human monocytes by extracellular ions and receptor density. Am J Physiol Cell Physiol 2001;280:C943–953. [PubMed: 11245611]

51. Rozengurt E, Heppel LA. A Specific effect of external ATP on the permeability of transformed 3T3 cells. Biochem Biophys Res Commun 1975;67:1581–1588. [PubMed: 1039]

52. Rozengurt E, Heppel LA, Friedberg I. Effect of exogenous ATP on the permeability properties of transformed cultures of mouse cell lines. J Biol Chem 1977;252:4584–4590. [PubMed: 17602]

53. Rozengurt E, Heppel LA. Reciprocal control of membrane permeability of transformed cultures of mouse cell lines by external and internal ATP. J Biol Chem 1979;254:708–714. [PubMed: 762092]
54. Labasi JM, Petrushova N, Donovan C, McCurdy S, Lira P, Payette MM, Brissette W, Wicks JR, Audoly L, Gabel CA. Absence of the P2X7 receptor alters leukocyte function and attenuates an inflammatory response. J Immunol 2002;168:6436–6445. [PubMed: 12055263]
55. Netea MG, Nold-Petry CA, Nold MF, Joosten LA, Opitz B, van der Meer JH, van de Veerdonk FL, Ferwerda G, Heinhuis B, Devesa I, Funk CJ, Mason RJ, Kullberg BJ, Rubartelli A, Van der Meer JW, Dinarello CA. Differential requirement for the activation of the inflammasome for processing and release of IL-1{beta} in monocytes and macrophages. Blood 2009;113:2324–2335. [PubMed: 19104081]
56. Gonnord P, Delarasse C, Auger R, Benihoud K, Prigent M, Cuif MH, Lamaze C, Kanellopoulos JM. Palmitoylation of the P2X7 receptor, an ATP-gated channel, controls its expression and association with lipid rafts. FASEB J 2009;23:795–805. [PubMed: 18971257]
57. Takenouchi T, Sato M, Kitani H. Lysophosphatidylcholine potentiates Ca2+ influx, pore formation and p44/42 MAP kinase phosphorylation mediated by P2X7 receptor activation in mouse microglial cells. J Neurochem 2007;102:1518–1532. [PubMed: 17437542]
58. Adriouch S, Hubert S, Pechberty S, Koch-Nolte F, Haag F, Seman M. NAD+ released during inflammation participates in T cell homeostasis by inducing ART2-mediated death of naive T cells in vivo. J Immunol 2007;179:186–194. [PubMed: 17579037]
59. Krebs C, Adriouch S, Braasch F, Koestner W, Leiter EH, Seman M, Lund FE, Oppenheimer N, Haag F, Koch-Nolte F. CD38 controls ADP-ribosyltransferase-2-catalyzed ADP-ribosylation of T cell surface proteins. J Immunol 2005;174:3298–3305. [PubMed: 15749861]
60. Taylor SR, Gonzalez-Begne M, Sojka DK, Richardson JC, Sheardown SA, Harrison SM, Pusey CD, Tam FW, Elliott JI. Lymphocytes from P2X7-deficient mice exhibit enhanced P2X7 responses. J Leukoc Biol. 2009(ePub ahead of print Mar 10, 2009)
61. Vial C, Roberts JA, Evans RJ. Molecular properties of ATP-gated P2X receptor ion channels. Trends Pharmacol Sci 2004;25:487–493. [PubMed: 15559251]
62. Marquez-Klaka B, Rettinger J, Bhargava Y, Eisele T, Nicke A. Identification of an intersubunit cross-link between substituted cysteine residues located in the putative ATP binding site of the P2X1 receptor. J Neurosci 2007;27:1456–1466. [PubMed: 17287520]
63. Marquez-Klaka B, Rettinger J, Nicke A. Inter-subunit disulfide cross-linking in homomeric and heteromeric P2X receptors. Eur Biophys J 2009;38:329–338. [PubMed: 18427801]
64. Rassendren F, Buell GN, Virginio C, Collo G, North RA, Surprenant A. The permeabilizing ATP receptor, P2X7. Cloning and expression of a human cDNA. J Biol Chem 1997;272:5482–5486. [PubMed: 9038151]
65. Haag F, Koch-Nolte F, Kuhl M, Lorenzen S, Thiele HG. Premature stop codons inactivate the RT6 genes of the human and chimpanzee species. J Mol Biol 1994;243:537–546. [PubMed: 7966280]
66. Donnelly LE, Rendell NB, Murray S, Allport JR, Lo G, Kefalas P, Taylor GW, MacDermot J. Arginine-specific mono(ADP-ribosyl)transferase activity on the surface of human polymorphonuclear neutrophil leucocytes. Biochem J 1996;315(Pt 2):635–641. [PubMed: 8615841]
67. Paone G, Wada A, Stevens LA, Matin A, Hirayama T, Levine RL, Moss J. ADP ribosylation of human neutrophil peptide-1 regulates its biological properties. Proc Natl Acad Sci U S A 2002;99:8231–8235. [PubMed: 12060767]
68. Balducci E, Horiba K, Usuki J, Park M, Ferrans VJ, Moss J. Selective expression of RT6 superfamily in human bronchial epithelial cells. Am J Respir Cell Mol Biol 1999;21:337–346. [PubMed: 10460751]
69. Balducci E, Micossi LG, Soldaini E, Rappuoli R. Expression and selective up-regulation of toxin-related mono ADP-ribosyltransferases by pathogen-associated molecular patterns in alveolar epithelial cells. FEBS Lett 2007;581:4199–4204. [PubMed: 17707376]
70. Braren R, Glowacki G, Nissen M, Haag F, Koch-Nolte F. Molecular characterization and expression of the gene for mouse NAD+:arginine ecto-mono(ADP-ribosyl)transferase, Art1. Biochem J 1998;336(Pt 3):561–568. [PubMed: 9841866]

71. Hong S, Brass A, Seman M, Haag F, Koch-Nolte F, Dubyak GR. Basal and inducible expression of the thiol-sensitive ART2.1 ecto-ADP-ribosyltransferase in myeloid and lymphoid leukocytes. Purinergic Signal. 2009(ePub ahead of print Apr 30, 2009)

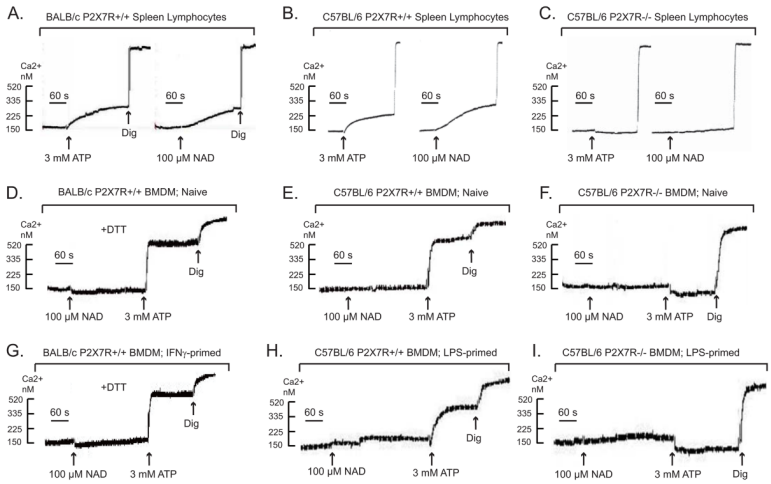

Figure 1. NAD induces activation of P2X7R in murine lymphocytes but not murine macrophages

Changes in cytosolic Ca^{2+} in response to ATP (3 mM) or NAD (100 μM) were measured in fura 2-loaded suspensions of spleen lymphocytes or bone marrow-derived macrophages (BMDM) as described in methods. Macrophage suspensions were pre-treated with a cocktail of 50 μM ADP and 50 μM UTP to activate and desensitize P2Y receptors 5 min prior to P2X7R stimulation by ATP or NAD. Where indicated, 1 mM DTT was included in the assay medium to support activity of the thiol-sensitive ART2.1 ecto-enzyme. All cells were permeabilized with digitonin (dig) to release fura-2 for subsequent calibration. All traces are representative of observations from 3–6 experiments with the leukocyte preparations isolated from different mice of the noted strains.

A) Freshly isolated spleen lymphocytes from BALB/c mice. B) Freshly isolated spleen lymphocytes from C57BL/6 mice. C) Freshly isolated spleen lymphocytes from the spleen of P2X7R-knockout mice (C57BL/6 background). D) Naive BMDM from BALB/c mice. E) Naive BMDM from C57BL/6 mice. F) Naive BMDM from P2X7R-knockout mice (C57BL/6 background). G) BMDM from BALB/c mice were primed with 100 U/ml IFN-γ for 24 h to induced ART2.1 expression before the Ca^{2+} assay. H) BMDM from C57BL/6 BMDM were primed with 100 ng/ml LPS plus 10 μM U0126 for 24 h to induce proinflammatory gene expression before the Ca^{2+} assay. I) BMDM from P2X7R-knockout mice (C57BL/6 background) were primed with 100 ng/ml LPS plus 10 μM U0126 for 24 h to induce proinflammatory gene expression before the Ca^{2+} assay.

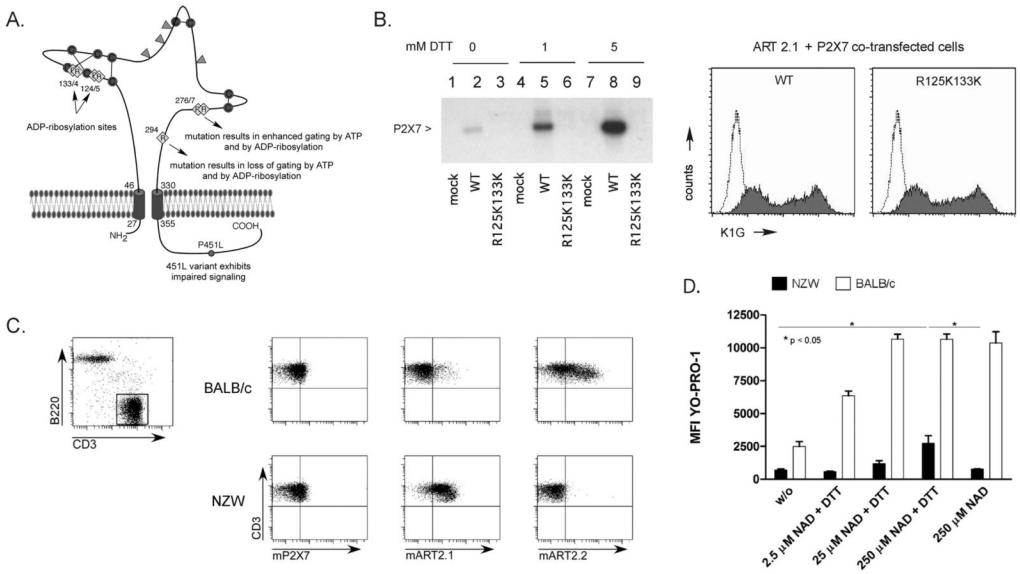

Figure 2. The murine P2X7R is a substrate for ADP-ribosylation and gating by both the thiol-sensitive ART2.1 and the thiol-insensitive ART2.2

A) Schematic of murine P2X7R showing the relative distribution of important arginine residues (yellow), disulfide-bonded cysteine residues (red), and N-linked glycosylation sites (green) in the extracellular ligand-binding domain, as well as the natural allelic 451L variant in the cytosolic domain of P2X7R. B) HEK cells were co-transfected with wildtype murine P2X7R (WT) plus murine ART2.1, or with an R125K/R133K double mutant of the murine P2X7R (R125K133K) plus murine ART2.1. Aliquots of the control and transfected cells were stained with the anti-P2X7 K1G Ab for FACS analysis as described in Methods. Parallel aliquots of the control (mock-tranfected) or co-transfected cells were incubated for 15 min with 50 μM [^{32}P]-NAD and 1 mM ADP-R in the presence of the indicated concentrations of DTT prior to lysis and immunoprecipitation with the K1G Ab; immunoprecipitated products were resolved by SDS-PAGE and detected by autography. Results are representative of observations from 2 or more independent experiments. C) FACS analysis of splenocytes from BALB/c and NZW mice. CD3-expressing T lymphocytes (top panel) were analyzed for surface expression of P2X7R, ART2.1, and ART2.2 (bottom panels). D) Splenocytes were incubated with the fluorescent dye YO-PRO-1 and NAD and DTT as indicated. The mean fluorescence intensity in the YO-PRO-1 channel of cells gated for CD3 expression as in C was measured as an indication of pore formation in T lymphocytes. Data bars show the mean±SE of the MFI values from 3 independent experiments for each T cell type with $p < 0.05$ for the indicated comparisons in the NZW data sets.

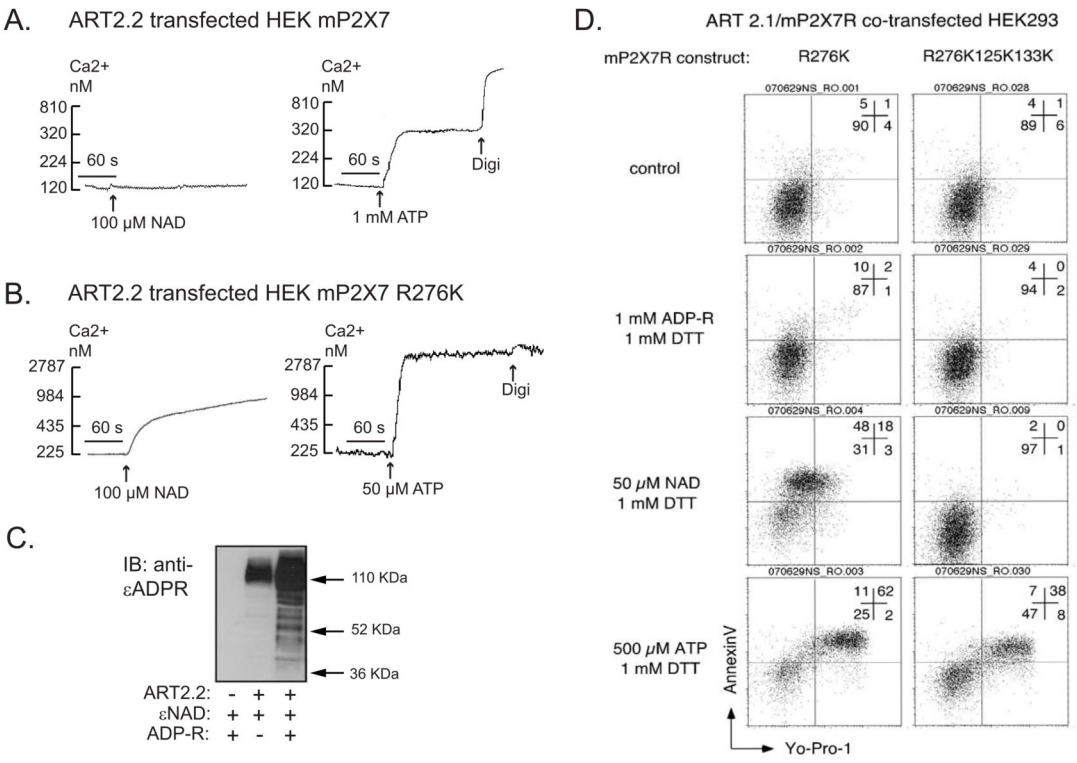

Figure 3. Differential effects of NAD/ART2 on activation of the murine P2X7R versus R276K mutated P2X7R in HEK293 cells

A, B) HEK293 cells were stably transfected with either wildtype murine P2X7R (HEK-mP2X7 cells) in panel A, or R276K mutant of murine P2X7R (HEK-mP2X7-R276K cells) in panel B. The stably transfected lines were transiently co-transfected with murine ART2.2 24 h prior to analysis of P2X7R-dependent Ca^{2+} influx. Cytosolic Ca^{2+} was measured in fura-2 loaded HEK cell suspensions as described in Methods and Figure 1. The cell suspensions were pre-treated with a cocktail of 50 μM ADP and 50 μM UTP to activate and desensitize P2Y receptors 5 min prior to P2X7R stimulation by the indicated concentrations of ATP or NAD. NAD was added together with 1 mM ADP-R to attenuate metabolism of the NAD. These traces are representative of observations from 3–4 experiments with each cell line. C) HEK293 cells were transiently mock-transfected (lane 1) or transfected with ART2.2 (lanes 2 and 3). After 36 h, the intact cells were acutely incubated for 15 min with 50 μM ε-NAD plus or minus 1 mM ADP-ribose prior to extraction, SDS-PAGE, and western blotting with the 1G4 mAb that detects ε-ADP-ribosylated proteins. D) HEK cells were transiently co-transfected with murine ART2.1 and the indicated murine P2X7R mutants (R276K single mutant or R125K/R133K/R276K triple mutant) before experiments. At 20 h post-transfection, the cells were harvested by trypsinization without further treatment (control) or following 10-minute incubations with 1 mM ADP-R, 50 μM NAD or 500 μM ATP separately in the presence of 1 mM DTT. The cells were then treated with 1 μM YO-PRO-1 for 1 hour. Aliquots of the co-transfected cells were stained with APC-conjugated annexin V before FACS analysis. All results are representative of observations from 2 or more independent experiments. The numbers in each panel represent the percentages of cells in the respective quadrants.

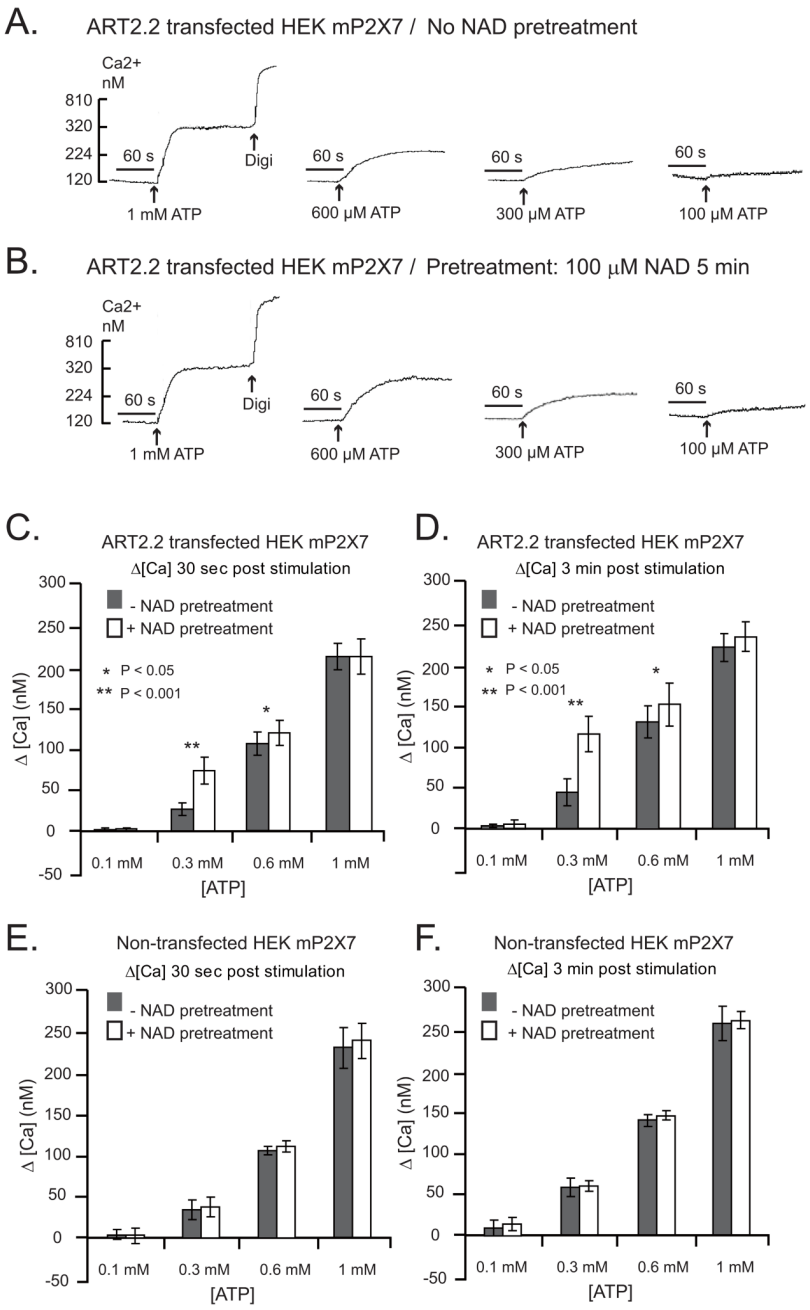

Figure 4. NAD potentiates ATP-induced P2X7R activation in HEK293 cells co-expressing ART2 and P2X7R

HEK293 cells stably transfected with wildtype murine P2X7R (HEK-mP2X7 cells) were used in all experiments. In experiments for panels A-D, the cells were transiently co-transfected with murine ART2.2 24 h prior to analysis of P2X7R-dependent Ca^{2+} influx. In experiments for panels E-F, the HEK-mP2X7 cells that lack ART2.2 expression were directly assayed. Cytosolic Ca^{2+} was measured in fura2-loaded HEK cell suspensions as described in Figure 3. The cell suspensions were pre-treated with a cocktail of 50 μM ADP and 50 μM UTP to activate and desensitize P2Y receptors 5 min prior to P2X7R stimulation by the indicated concentrations of ATP; where indicated (as in the panel B traces) 100 μM NAD (plus ADP-R) was also added 5 min prior addition of ATP. In each assay, the cells were permeabilized with digitonin (digi)

for calibration of Ca^{2+-} dependent fura-2 fluorescence. A, B) ATP-induced Ca^{2+} influx without (panel A) or with (panel B) NAD pre-treatment for 5 min. These traces are representative of observations from 4 experiments. C, D) Changes in cytosolic Ca^{2+} in ART2.2 transfected cells were quantified at 30 s (panel C) or 3 min (panel) after addition of the indicated concentration of ATP with or without NAD pretreatment. Data bars represent the mean±SE from 4 experiments. E, F) Identical experiments as in panels C and D, but with HEK-mP2X7 cells not transfected with ART2.2. Data bars represent the mean±SE from 3 experiments.

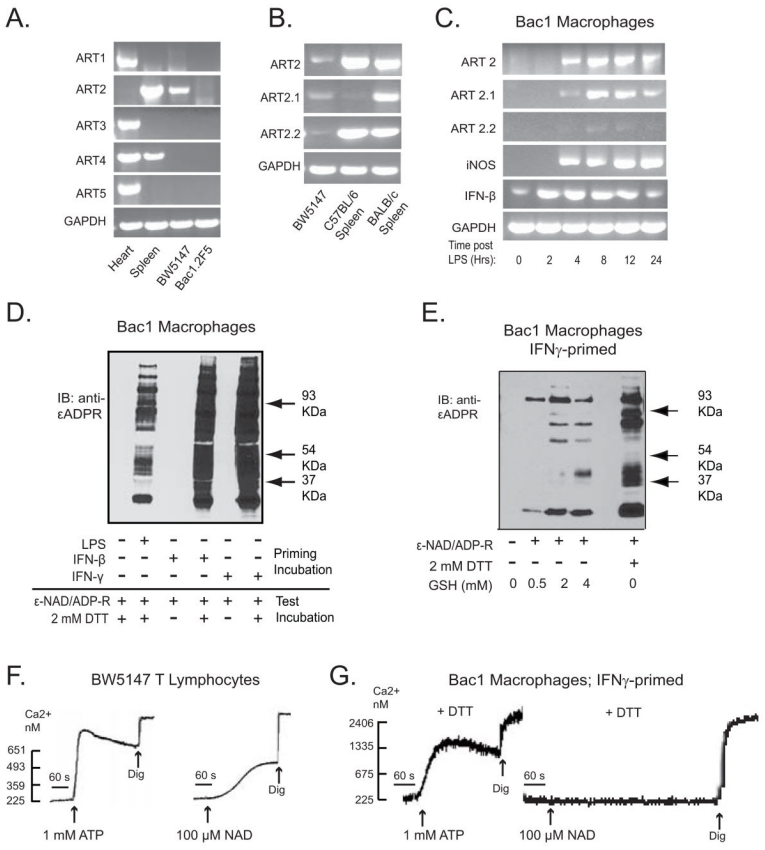

Figure 5. Differential effects of NAD/ART2 on P2X7R function in established murine macrophage and T lymphocyte cell lines

A) Expression of ART1, 2, 3, 4, or 5 mRNA was assayed by RT-PCR in BW5147 lymphocytes and Bac1.2F5 macrophages, as well as in freshly isolated extracts of heart or spleen from a BALB/c mouse. B) RT-PCR analysis for total ART2, ART2.1 ART2.2 in BW5147 cells and freshly isolated spleen tissues from BALB/c or C57BL/6 mice. C) Bac1.2F5 macrophages were transferred to M-CSF-free medium and stimulated with LPS (100 ng/ml) for the indicated times prior to extraction and RT-PCR analysis for ART2, ART2.1, ART2.2, iNOS, IL-1β, or GAPDH content. D) Bac1.2F5 macrophages were transferred to M-CSF-free medium and stimulated with or without IFN-β (100 U/ml), IFN-γ (100 U/ml) or LPS (100 ng/ml) for 24 hours (priming incubation). The primed cells were then stimulated with 50 μM ε-NAD and 1 mM ADP-R in the presence or absence of 2 mM DTT at 37°C for 15 minutes (test incubation) prior to extraction for SDS-PAGE and western blot analysis of 1G4 reactive εADP-ribosylated proteins. E) Bac1.2F5 macrophages were stimulated with or without IFN-γ (100 U/ml) for 24 hours. The primed cells were then stimulated with 50 μM ε-NAD and 1 mM ADP-R in the presence or absence of the indicated concentrations of GSH or DTT at 37°C for 15 minutes. F, G) ATP- or NAD-induced changes in Ca^{2+} was assayed in fura2-loaded suspensions of untreated BW5147 T lymphocytes (panel F) or Bac1.2F5 macrophages primed for 24 h with IFN-γ (panel G). For Bac1 cells, the 100 μM NAD was added together 1 mM ADP-R and 1 mM DTT. These results are representative of observations from 3 or more experiments.

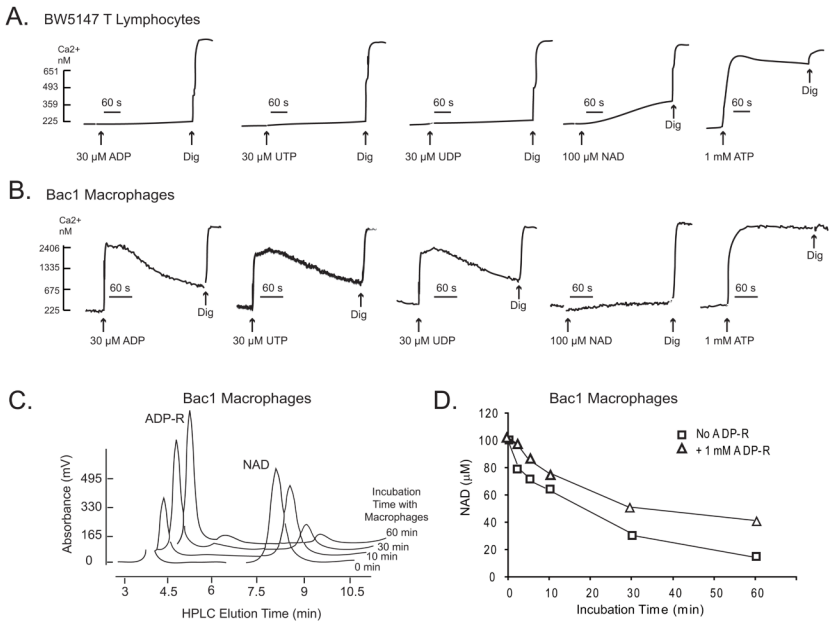

Figure 6. P2Y receptor-based Ca^{2+} signaling and extracellular NAD metabolism in murine macrophage and T lymphocyte cell lines

A, B. Cytosolic Ca^{2+} was assayed in fura 2-loaded suspensions of BW5147 T cells (panel A) or IFN-γ primed Bac1.2F5 macrophages (panel B) challenged with the indicated concentrations of ADP, UTP, UDP, NAD, or ATP. The results are representative of observations from 2 experiments. C, D. Monolayers of Bac1.2F5 macrophages (10^6 cells/well in 6-well dishes) were incubated in 1 ml BSS at 37°C supplemented with 100 μM NAD in the presence or absence of 1 mM ADP-ribose. At selected times (0–60 min), 100 μl aliquots of the extracellular medium were removed and processed for HPLC analysis. Panel C. Stacked HPLC chromatograms of extracellular samples taken at the 0, 10, 30, and 60 min timepoints. Panel D. NAD concentrations at the indicated times were calculated from the HPLC chromatograms.

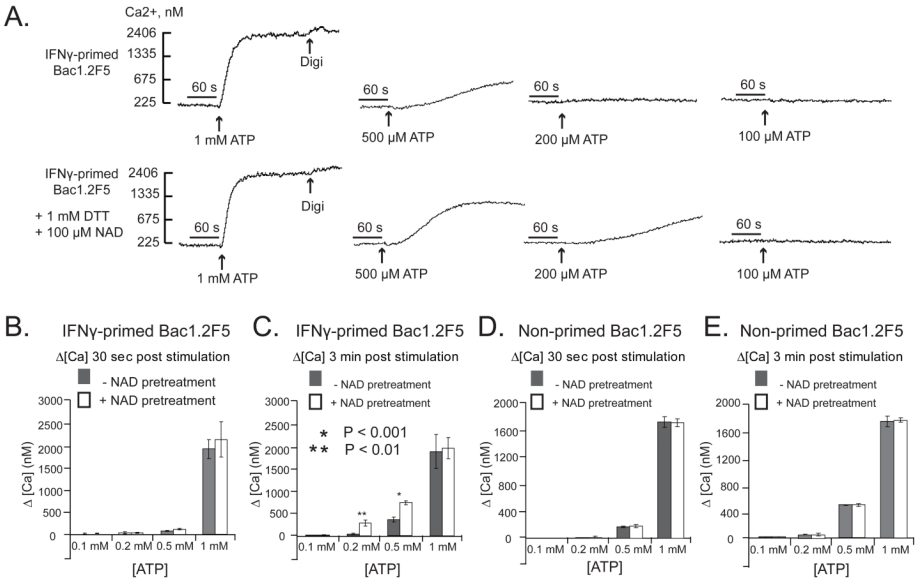

Figure 7. NAD potentiates ATP-induced P2X7R activation in interferon-primed murine macrophages that express ART2.1

Bac1.2F5 macrophages were transferred to M-CSF-free medium and then stimulated with IFN-γ (100 U/ml) for 24 hr (Panels A-C) or were incubated in M-CSF-free medium 24 hr in the absence of IFN-γ. Cytosolic Ca^{2+} was measured in fura-2 loaded Bac1 cell suspensions as previously described but with inclusion of 1 mM DTT and 1 mM ADP-R in all test media. The cell suspensions were pre-treated with a cocktail of 50 μM ADP and 50 μM UTP to activate and desensitize P2Y receptors 5 min prior to P2X7R stimulation by the indicated concentrations of ATP; where indicated (as in the panel B traces) 100 μM NAD was also added 5 min prior addition of ATP. In each assay, the cells were permeabilized with digitonin (digi) for calibration of Ca^{2+-} dependent fura-2 fluorescence. A) ATP-induced Ca^{2+} influx without or with NAD pre-treatment for 5 min. These traces are representative of observations from 4 experiments. B, C) Changes in cytosolic Ca^{2+} in IFN-γ-primed Bac1 macrophages were quantified at 30 s (panel B) or 3 min (panel C) after addition of the indicated concentration of ATP with or without NAD pretreatment. Data bars represent the mean±SE from 4 experiments. D, E) Identical experiments as in panels B and C, but with Bac1 macrophages that were not primed with IFN-γ. Data bars represent the mean±SE from 4 experiments.

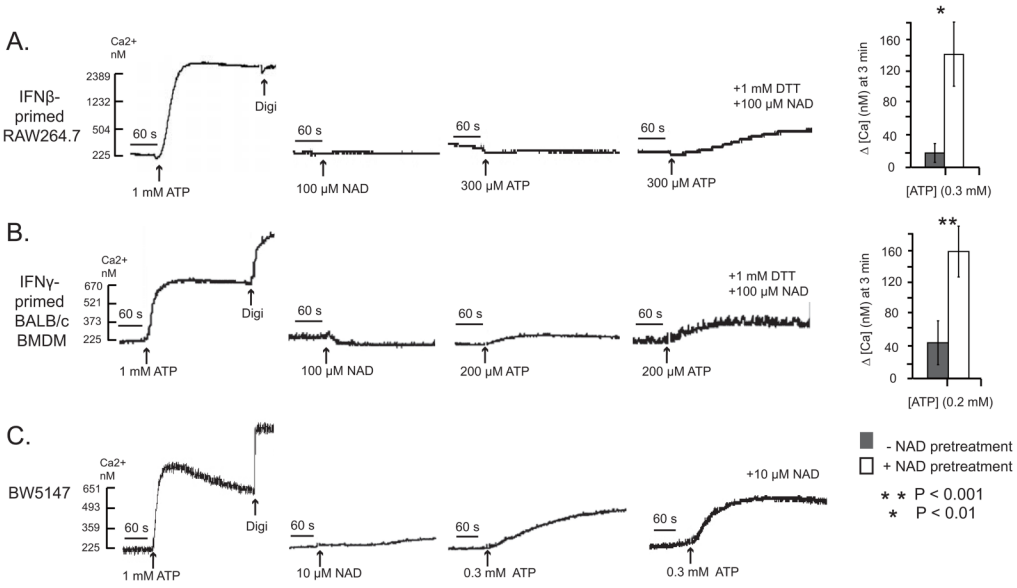

Figure 8. Comparative effects of NAD on potentiation of ATP-induced P2X7R activation in primary macrophages, a macrophage cell line, and a T-cell line

Experiments similar to those described in Figure 6 with Bac1.2F5 macrophages were performed using other murine leukocytes that express P2X7R. A) RAW264.7 macrophages were transferred to M-CSF-free medium and stimulated with IFN-β (100 U/ml) for 24 hr. The primed macrophages were stimulated with 1 mM ATP alone, 100 μM NAD (plus DTT) alone, or with 300 μM ATP in the absence or presence of a pretreatment with 100 μM NAD (plus DTT) for 5 min. The accompanying histograms (mean±SE from 3 experiments) show the quantified changes in Ca^{2+} at 3 min after addition of 300 μM ATP with and without NAD pretreatment. B) BALB/c BMDM were transferred to M-CSF-free medium and stimulated with IFN-γ (100 U/ml) for 24 h. The cells were stimulated and assayed as described in (A) but 200 μM ATP as the test pulse. The accompanying histograms (mean±SE from 3 experiments) show the quantified changes in Ca^{2+} at 3 min after addition of 200 μM ATP with and without NAD pretreatment. C) BW5147 T lymphocytes were stimulated with 1 mM ATP alone, 10 μM NAD alone, or with 300μM ATP in the absence or presence of a pretreatment with 10 μM NAD for 5 min. These results are representative of observations from 3 experiments.

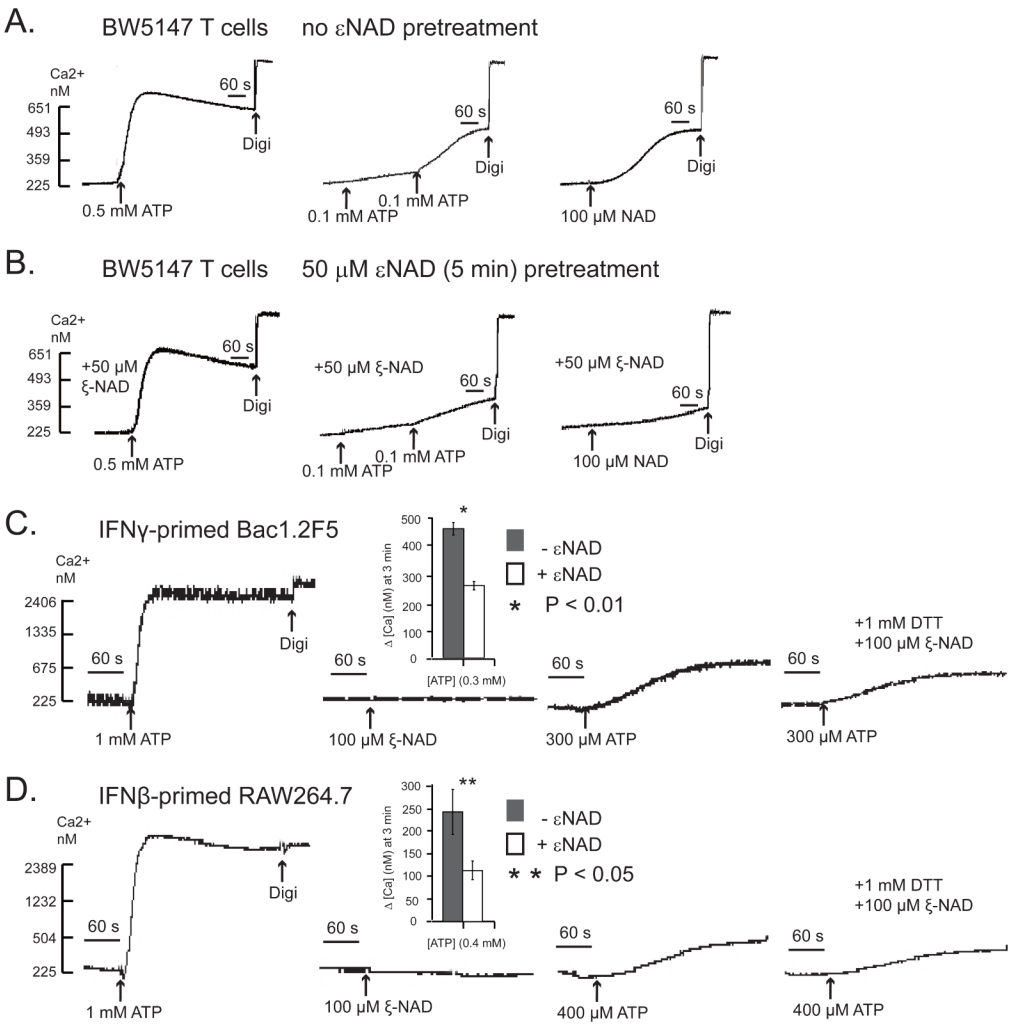

Figure 9. ε-NAD, an NAD analog, desensitizes P2X7R to ATP in macrophages and T lymphocytes

Experiments similar to those described in Figure 7 were performed but using the NAD analog,εNAD, as the ART2 substrate for pretreatment of murine leukocytes that express P2X7R. A) BW5147 T lymphocytes were stimulated with 0.5 mM ATP alone, 200 μM ATP alone (added as two sequential 100 μM pulses), or 100 μM NAD alone. These results are representative of observations from 2 experiments. B) Identical experiment as in panel A but with BW5147 T lymphocytes that were pretreated with 50 μM εNAD for 5 min prior to stimulation with 0.5 mM ATP alone, 200 μM ATP alone (added as two sequential 100 μM pulses), or 100 μM NAD alone. These results are representative of observations from 2 experiments. C) Bac1.2F5 macrophages were transferred to M-CSF-free medium and stimulated with IFN-γ (100 U/ml) for 24 h. The primed macrophages were acutely stimulated with 1 mM ATP alone, 100 μM εNAD (plus DTT) alone, or with 300 μM ATP in the absence or presence of a pretreatment with 100 μM εNAD (plus DTT) for 5 min. The accompanying histograms (mean±SE from 3 experiments) show the quantified changes in Ca^{2+} at 3 min after addition of 300 μM ATP with and without εNAD pretreatment. D) RAW264.7 macrophages were transferred to M-CSF-free medium and stimulated with IFN-β (100 U/ml) for 24 hr. The primed macrophages were acutely stimulated with 1 mM ATP alone, 100 μM εNAD (plus DTT) alone, or with 400 μM ATP in the absence or presence of a pretreatment with 100 μM εNAD (plus DTT) for 5 min. The accompanying histograms (mean±SE from 3 experiments)

show the quantified changes in Ca^{2+} at 3 min after addition of 400 μM ATP with and without εNAD pretreatment.

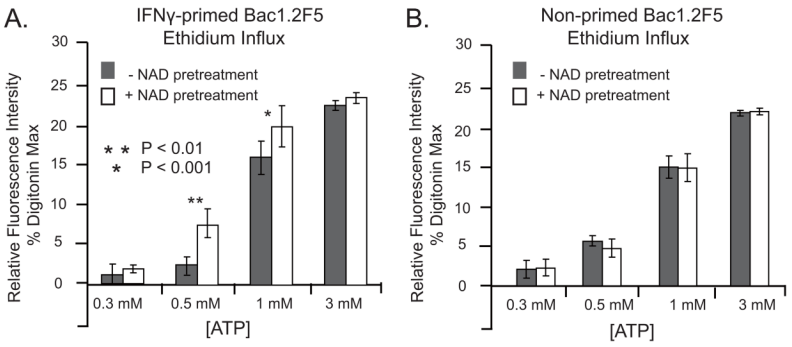

Figure 10. NAD potentiates ATP-induced pore formation in IFN-γ-primed murine macrophages

Bac1.2F5 macrophages were suspended in BSS and ATP-induced ethidium accumulation was assayed as described in Methods. A) Bac1.2F5 macrophages were transferred to M-CSF-free medium and stimulated with IFN-γ (100 U/ml) for 24 hr before assay of ethidium accumulation. The primed macrophages were stimulated with the indicated concentrations of ATP in the absence or presence of pretreatment with 100 μM NAD (plus 1 mM DTT) for 5 min prior to the addition of ATP. Accumulation of fluorescent ethidium/DNA/RNA complexes was measured at 350 sec after ATP addition. Data bars represent the mean±SE from 4 experiments.